

The Effect of Freeze-Thaw Cycles on the Basic Mechanical Properties of PVA-ECC Materials

Wenli Jiao*

School of Civil Engineering, Henan Polytechnic University, Jiaozuo, China

*Corresponding Author: Wenli Jiao

Abstract

To investigate the frost resistance and mechanical performance stability of Polyvinyl Alcohol Engineered Cementitious Composites (PVA-ECC) in cold regions, a series of rapid freeze-thaw tests were conducted on PVA-ECC specimens with four fiber volume contents (0%, 1.0%, 1.5%, and 2.0%). The effects of freeze-thaw cycles (0, 50, 100, 150, and 200 cycles) on the surface morphology, mass loss rate, relative dynamic elastic modulus, and cubic compressive strength of the specimens were systematically analyzed. The results indicate that freeze-thaw cycles cause cumulative damage to PVA-ECC, manifested as aggravated surface mortar spalling, increased mass loss, decreased relative dynamic elastic modulus, and degraded compressive strength. However, the incorporation of PVA fibers significantly improves the material's frost resistance and mechanical stability through the bridging effect and structural optimization. With the increase in fiber volume content, the damage degree of PVA-ECC under freeze-thaw cycles is remarkably reduced. After 200 freeze-thaw cycles, the specimen with 2.0% fiber content maintains an intact overall structure, with a mass loss rate of only 2.76%, a relative dynamic elastic modulus retention rate of 73.19%, and a cubic compressive strength of 31.73 MPa (strength loss rate of 30.26%). In contrast, the fiber-free specimen fractures after 75 freeze-thaw cycles, with a mass loss rate of 9.49% and a strength loss rate of 50.05%. This study demonstrates that PVA fibers can effectively inhibit the initiation and propagation of microcracks induced by freeze-thaw cycles, enhance the bonding stability between the matrix and fibers, and reduce internal structural damage. The findings provide experimental data and technical support for the application and popularization of PVA-ECC in cold-region engineering.

Keywords

PVA-ECC, Freeze-Thaw Cycles, Static Mechanical Properties, Frost Resistance, Compressive Strength.

1. Introduction

Since the advent of cement concrete in the 19th century, it has become the most widely used construction material globally due to its advantages such as convenient availability of raw materials, high compressive strength, and low cost^[1]. However, traditional concrete has inherent defects including low tensile strength, high brittleness, and susceptibility to cracking. Under the action of freeze-thaw cycles in cold regions, the repeated freezing and thawing of free water inside generate frost heave stress and osmotic pressure, leading to the initiation and propagation of microcracks. Eventually, this causes surface spalling and strength attenuation, which seriously affects the safety and durability of engineering structures^[2-3]. According to statistics, the area of seasonal permafrost regions in China reaches 5.13×10^6 km², accounting for 53.5% of the total national territory. Freeze-thaw damage has become the main inducement

for the premature failure of concrete structures in cold regions, resulting in huge economic losses every year^[4].

Engineered Fiber-Reinforced Cementitious Composites (ECC), as a high-performance cementitious material designed based on micromechanics, achieve strain hardening and multiple cracking characteristics by incorporating short-cut fibers, with an ultimate tensile strain 30 to 50 times that of ordinary concrete^[5]. Among various fibers, polyvinyl alcohol (PVA) fibers have emerged as an ideal reinforcing phase for ECC fabrication, attributed to their excellent bonding performance with the cement matrix, high tensile strength, and controllable cost. The resulting PVA-ECC material integrates high ductility, high durability, and favorable economy, thus holding significant application value in fields such as cold-region engineering repair and seismic-resistant structures^[6-7].

Most existing studies have focused on the mechanical properties of PVA-ECC under normal temperature conditions. In the cold regions of northern China, temperatures alternate around zero degrees Celsius during spring and winter, and concrete components have to withstand the action of freeze-thaw cycles for a long time. Therefore, investigating the influence of freeze-thaw cycles on the basic mechanical properties of PVA-ECC is of great engineering significance. Through a series of tests, this study reveals the coupling effect of freeze-thaw cycles and PVA fiber content on the mechanical properties of PVA-ECC from two aspects, namely frost resistance and static compressive performance, providing data support for its popularization and application in cold-region engineering.

2. Materials and Mix Proportion Design

2.1. Experimental Materials

The main raw materials of PVA-ECC are shown in Figure 1, including P.O 42.5 ordinary Portland cement; Grade I fly ash with a loss on ignition of 1.7%; sieved fine sand with a maximum particle size of ≤ 0.6 mm and a clay content of 0.65%; and PVA fibers.



Figure 1. PVA-ECC raw materials

In this study, P.O 42.5 ordinary Portland cement was used. Grade I fly ash produced by a thermal power plant was adopted, featuring a loss on ignition of 1.7%, a water demand ratio of 94%, and an apparent density of 2.1 g/cm^3 ; detailed specifications are presented in Table 1. Natural river sand, after sieving treatment, was selected as the fine aggregate, with a maximum particle size of ≤ 0.6 mm, and its specific parameters are shown in Table 2. A polycarboxylate

superplasticizer was employed to effectively improve the fluidity of PVA-ECC, prevent fiber agglomeration, and enhance the bonding performance between the matrix and fibers, with specific parameters provided in Table 3. Type K-II PVA fibers manufactured by Kuraray Co., Ltd. (Japan) were used, and their performance parameters are summarized in Table 4.

Table 1. Properties of fly ash

Fineness (%)	Water Demand (%)	Loss on Ignition (%)	SO ₃ Content (%)	Moisture Content (%)	Apparent Density (g/cm ³)	Soundness
4	94	1.7	0.2	<1	2.1	Compliant

Table 2. Properties of sands

Name	Apparent Density (kg/m ³)	Bulk Density (kg/m ³)	Clay Content (%)	Fineness Modulus	Particle Size (mesh)
Natural river sand	1650	1280	0.65	1.6	70-100

Table 3. Properties of Polycarboxylate Superplasticizer

Name	Color	Paste Fluidity (mm)	pH	Na ₂ SO ₄ Content (%)	Density (g/cm ³)
Polycarboxylate Superplasticizer	Pale Yellow	≤270	6.2-7.9	≤0.2	1

Table 4. Properties of PVA fibers

Diameter/μm	Length/mm	Tensile strength/MPa	Ultimate strain/%	Elastic modulus/GPa	Density/(g·cm ⁻³)
39	12	1620	7.0	42.8	1.2

2.2. Mix Proportion Design

Based on the previous research of the research group and combined with the workability and mechanical property requirements of PVA-ECC materials, four mix proportions with different PVA fiber volume contents (0%, 1.0%, 1.5%, and 2.0%) were designed, as detailed in Table 5. In the mix proportion design, the water-binder ratio was fixed at 0.36, the sand-binder ratio at 0.36, and the mass ratio of fly ash to cement at 1.22. The dosage of superplasticizer was adjusted according to the fiber content to ensure that the fluidity spread of the material was controlled between 120-160 mm, which meets the requirements for specimen preparation^[8].

Table 5. Mix ratio of PVA-ECC

Design Strength Grade	PVA Fiber Content (%)	Fly Ash (kg/m ³)	Cement (kg/m ³)	Sand-Binder Ratio	Water-Binder Ratio	Superplasticizer (%)
E40-0.0	0	680	555	0.36	0.36	1.20
E40-1.0	1.0	680	555	0.36	0.36	1.51
E40-1.5	1.5	680	555	0.36	0.36	1.64
E40-2.0	2.0	680	555	0.36	0.36	1.72

Note: E40-0.0 indicates that the designed strength grade of the specimen is 40 MPa with a fiber content of 0%; the PVA fiber content refers to the volume fraction; the superplasticizer content is the mass percentage of superplasticizer relative to cement, and the fluidity spread of the material is controlled within the range of 120 mm-160 mm.

2.3. Specimen Preparation and Curing

Prismatic specimens of 100 mm × 100 mm × 300 mm were used in the test for freeze-thaw cycle, mass loss, and relative dynamic elastic modulus measurements, while cubic specimens of 70.7 mm × 70.7 mm × 70.7 mm were employed for compressive strength testing. Three parallel specimens were set for each fiber content and each freeze-thaw cycle number, resulting in a total of 60 cubic specimens and 120 specimens in total.

Cement, fly ash, fine sand, water, PVA fibers, and superplasticizer were accurately weighed according to the mix proportion, with the weighing accuracy controlled within $\pm 1\%$. Cement, fly ash, and fine sand were poured into a UJZ-15 mortar mixer and dry-mixed for 3 minutes until uniformly blended. Subsequently, the mixed solution of water and superplasticizer was added, followed by wet-mixing for 3 minutes. Finally, PVA fibers were slowly added, and mixing was continued for 6–8 minutes to ensure uniform dispersion of fibers without agglomeration. The uniformly mixed PVA-ECC mixture was then poured into molds in two batches. After each pouring, the mold was vibrated on a vibration table for 40–50 seconds to remove internal air bubbles and ensure specimen compactness. After pouring, the surface was smoothed with a trowel and covered with a plastic film to prevent moisture evaporation. The specimens were first cured at room temperature (20 ± 2) °C with a relative humidity of $\geq 90\%$ for 24 hours before demolding. They were then transferred to a standard curing room (temperature: 20 ± 2 °C, relative humidity: $\geq 95\%$) for 24 days. Afterwards, the specimens to be subjected to freeze-thaw cycles were immersed in tap water for 4 days to ensure complete water saturation prior to the freeze-thaw cycle test; the non-freeze-thaw specimens were continuously cured under standard conditions until 28 days.

The TDR-28 rapid freeze-thaw testing machine was adopted, and the test was conducted in accordance with the rapid freeze-thaw method specified in the national standard GB/T 50082-2009 "Standard for Test Methods of Long-Term Performance and Durability of Ordinary Concrete". The temperature of the freeze-thaw cycle was controlled within the range of (-18 ± 2) °C to (5 ± 2) °C, with a cycle period of 2.5–4 hours, and the thawing time was not less than 1/4 of the cycle. The freeze-thaw cycle numbers were set as 0, 50, 100, 150, and 200. Every 25 freeze-thaw cycles, the specimens were taken out for surface morphology observation, mass weighing, and wave velocity testing^[9], as shown in Figure 2. The freeze-thaw test was terminated when the specimens met any of the following conditions: the freeze-thaw cycle number reached the designed value; the mass loss rate was $\geq 5\%$; the relative dynamic elastic modulus loss rate was $\geq 40\%$. After the freeze-thaw cycles, the surfaces of the cubic specimens were wiped dry, and the compressive strength test was performed using a YNS-600 microcomputer-controlled electro-hydraulic servo universal testing machine.



Figure 2. Velocity measurement

3. Test Results and Analysis

3.1. Surface Morphology

The changes in surface morphology of PVA-ECC specimens under different freeze-thaw cycles and PVA fiber volume contents are shown in Figure 3.

At 0 freeze-thaw cycles (unfrozen): All specimens exhibited a flat and smooth surface without mortar spalling, cracks, or fiber exposure. The fiber-free specimen (PVA0-0) had a dense surface. For specimens containing PVA fibers (PVA1.0-0, PVA1.5-0, PVA2.0-0), no fiber exposure was observed, the matrix and fibers bonded well, and only a small number of tiny air bubbles existed locally.

At 50 freeze-thaw cycles: The fiber-free specimen (PVA0-50) became porous with severe mortar spalling, obvious corner damage, and multiple irregular cracks. The PVA1.0-50 specimen showed a few surface pores and slight mortar spalling without significant fiber exposure. The PVA1.5-50 and PVA2.0-50 specimens maintained relatively intact surfaces with a small number of small-diameter pores, insignificant mortar spalling, and no fiber exposure.

At 75 freeze-thaw cycles: The fiber-free specimen (PVA0-75) fractured in the middle, with extensive surface mortar spalling and complete corner damage; it could be easily broken. The mass loss rate reached 9.49%, meeting the test termination condition and exiting subsequent freeze-thaw cycles. Among fiber-reinforced specimens, the PVA1.0-75 specimen had increased surface pores and aggravated mortar spalling. The PVA1.5-75 and PVA2.0-75 specimens still maintained good surface integrity with only slight mortar spalling at the corners and no fracture.

At 100 freeze-thaw cycles: The PVA1.0-100 specimen suffered severe mortar spalling, obvious corner damage, extensive fiber exposure, and some fibers bonded with mortar particles. The PVA1.5-100 specimen had an increased number of surface pores and cracks with mild fiber exposure. The PVA2.0-100 specimen remained relatively intact with minimal fiber exposure, and mortar spalling was mainly concentrated at the corners.

At 150 freeze-thaw cycles: The PVA1.0-150 specimen showed crack propagation and penetration, expanded mortar spalling area, and further increased fiber exposure. The PVA1.5-150 specimen had developed pores and cracks with moderate mortar spalling. The PVA2.0-150 specimen only had a few fine cracks, slight mortar spalling, and obvious fiber bridging effect, which inhibited crack propagation.

At 200 freeze-thaw cycles: The PVA1.0-200 specimen experienced extensive mortar spalling, crack penetration, massive fiber exposure, and partial fiber pull-out, resulting in decreased overall integrity. The PVA1.5-200 specimen had numerous cracks and pores with obvious mortar spalling but no fracture. The PVA2.0-200 specimen maintained good overall integrity with only corner mortar spalling, mild fiber exposure, a small number of pores, and no penetrating cracks.

The essential cause of surface morphology damage to PVA-ECC induced by freeze-thaw cycles is the combined effect of internal frost heave stress and osmotic pressure^[10]. In the early stage of freeze-thaw cycles, water in capillary pores and gel pores of the specimens freezes, generating frost heave stress that initiates microcracks. During the thawing phase, cracks absorb water, providing conditions for the next frost heave. With the increase in freeze-thaw cycles, microcracks continue to propagate and penetrate, leading to surface mortar spalling and fiber exposure. Fiber-free specimens lack bridging effect, resulting in unconstrained crack propagation and eventual fracture. In contrast, the random distribution of PVA fibers can span cracks, transfer stress through interfacial bond strength, inhibit crack propagation and pore penetration, and reduce mortar spalling. Higher fiber content enhances the bridging effect, leading to milder surface morphology damage^[11].



PVA0-0



PVA1.0-0



PVA1.5-0



PVA2.0-0



PVA0-50



PVA1.0-50



PVA1.5-0



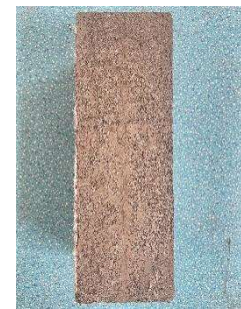
PVA2.0-50



PVA0-75



PVA1.0-75



PVA1.5-75



PVA2.0-75



PVA1.0-100



PVA1.5-100



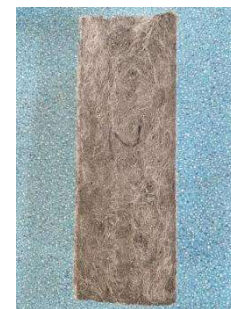
PVA2.0-100



PVA1.0-150



PVA1.5-150



PVA2.0-150



Figure 3. PVA-ECC freeze-thaw appearance damage example diagram

3.2. Mass Loss

The test results of the mass loss rate of PVA-ECC specimens under different freeze-thaw cycles and PVA fiber volume contents are presented in Figure 4. The mass loss rate increased with the increase in freeze-thaw cycles. The fiber-free specimen (PVA0) exhibited the most rapid growth in mass loss rate, reaching 3.12% after 25 freeze-thaw cycles, exceeding 5% after 50 cycles, and 9.49% after 75 cycles. In contrast, the mass loss rate of fiber-reinforced specimens increased relatively gently. After 200 freeze-thaw cycles, the mass loss rates of PVA1.0, PVA1.5, and PVA2.0 specimens were 3.95%, 3.42%, and 2.76%, respectively, none of which exceeded 5%. At the same number of freeze-thaw cycles, the mass loss rate decreased with the increase in fiber volume content. After 75 freeze-thaw cycles, the mass loss rates of PVA1.0, PVA1.5, and PVA2.0 specimens were 1.97%, 1.80%, and 0.79%, respectively, which were significantly lower than that of the PVA0 specimen (9.49%). After 200 freeze-thaw cycles, the mass loss rate of the specimen with 2.0% fiber content was 30.13% lower than that of the specimen with 1.0% fiber content. The mass loss rate of fiber-reinforced specimens increased rapidly in the early stage of freeze-thaw cycles (0–50 cycles) and then slowed down. A slight sudden increase in mass loss rate was observed for PVA1.0 and PVA1.5 specimens between 50 and 75 freeze-thaw cycles, which was attributed to the accumulation of freeze-thaw damage reaching a critical value, leading to concentrated surface mortar spalling. However, the sudden increase in mass loss rate of the PVA2.0 specimen occurred after 150 freeze-thaw cycles, indicating that a higher fiber content can delay the occurrence of concentrated mortar spalling.

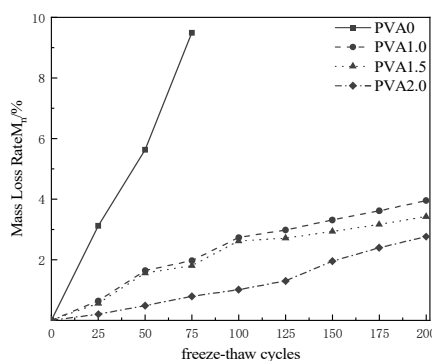


Figure 4. Mass loss rate of PVA-ECC specimens

The mass loss of PVA-ECC is mainly caused by surface mortar spalling and internal pore water evaporation induced by freeze-thaw cycles^[12]. During the freeze-thaw process, internal frost heave stress initiates microcracks, reducing the bond strength between mortar and the matrix. With the increase in cycles, crack propagation leads to mortar spalling and subsequent mass loss. Meanwhile, the evaporation of internal pore water in specimens during freeze-thaw cycles

also causes a small amount of mass loss. Fiber-free specimens suffer from unconstrained crack propagation, resulting in severe mortar spalling and a high mass loss rate. PVA fibers inhibit crack propagation through the bridging effect, enhance the bonding stability between mortar and the matrix, and reduce mortar spalling, thereby decreasing the mass loss rate. A higher fiber content results in a stronger bridging effect and lower mass loss^[13].

3.3. Relative Dynamic Elastic Modulus

The test results of the relative dynamic elastic modulus of PVA-ECC specimens under different freeze-thaw cycles and PVA fiber volume contents are presented in Figure 5. The relative dynamic elastic modulus decreased with the increase in freeze-thaw cycles. The fiber-free specimen (PVA0) exhibited the most significant decline, dropping to 89.91% after 25 freeze-thaw cycles, only 61.63% after 50 cycles, and becoming untestable after 75 cycles due to fracture. In contrast, the fiber-reinforced specimens showed a relatively gentle decrease. After 200 freeze-thaw cycles, the relative dynamic elastic moduli of PVA1.0, PVA1.5, and PVA2.0 specimens were 62.57%, 69.89%, and 73.19%, with relative dynamic elastic modulus loss rates of 37.43%, 30.11%, and 26.81%, respectively. At the same number of freeze-thaw cycles, the relative dynamic elastic modulus increased with the increase in fiber volume content. After 50 freeze-thaw cycles, the relative dynamic elastic moduli of PVA1.0, PVA1.5, and PVA2.0 specimens were 43.76%, 49.49%, and 54.21% higher than that of the PVA0 specimen (61.63%), respectively. After 200 freeze-thaw cycles, the relative dynamic elastic modulus of the specimen with 2.0% fiber content was 16.97% higher than that of the specimen with 1.0% fiber content. The decline rate of relative dynamic elastic modulus accelerates as the number of freeze-thaw cycles increases. The fiber-reinforced specimens showed a gentle decline in relative dynamic elastic modulus during 0–100 freeze-thaw cycles, and the decline rate accelerated after 100 cycles. This is attributed to the extensive propagation and penetration of internal cracks in the later stage of freeze-thaw cycles, which aggravated the looseness of the internal structure of the specimens, leading to a significant decrease in wave velocity^[14].

The relative dynamic elastic modulus is an important indicator reflecting the degree of internal damage to materials, and it is closely related to internal porosity and crack development status^[15]. In the early stage of freeze-thaw cycles, a small number of microcracks and pores are generated inside the specimens, resulting in a gentle decrease in wave velocity and a slight reduction in relative dynamic elastic modulus. With the increase in freeze-thaw cycles, microcracks continue to propagate and penetrate, the porosity increases, and the internal structure of the specimens becomes loose, leading to a significant decrease in wave velocity and a sharp reduction in relative dynamic elastic modulus. The incorporation of PVA fibers can inhibit crack propagation and pore penetration through the bridging effect, maintain the integrity of the internal structure of the specimens, and thus slow down the decline in relative dynamic elastic modulus. A higher fiber content results in a more significant inhibitory effect^[16].

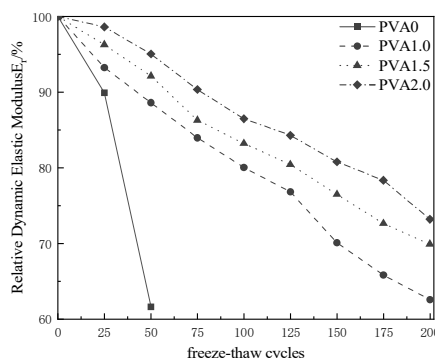


Figure 5. Relative Dynamic Elastic Modulus Diagram of PVA-ECC Specimens

3.4. Cubic Compressive Strength

The test results of the cubic compressive strength of PVA-ECC specimens under different freeze-thaw cycles and PVA fiber volume contents are presented in Figure 6. The cubic compressive strength degraded with the increase in freeze-thaw cycles. The fiber-free specimen exhibited the most severe degradation: after 50 freeze-thaw cycles, its strength decreased to 26.16 MPa with a loss rate of 34.93%; after 75 cycles, the strength was only 20.08 MPa with a loss rate of 50.05%, and it could no longer bear the load. In contrast, the strength degradation of fiber-reinforced specimens was relatively gentle. After 200 freeze-thaw cycles, the strengths of PVA1.0, PVA1.5, and PVA2.0 specimens were 27.12 MPa, 28.83 MPa, and 31.73 MPa, respectively, which were 35.55%, 34.25%, and 30.26% lower than those in the unfrozen state. At the same number of freeze-thaw cycles, the cubic compressive strength increased with the increase in fiber volume content. At 0 freeze-thaw cycles, the strengths of PVA1.0, PVA1.5, and PVA2.0 specimens were 4.68%, 9.08%, and 13.18% higher than that of the PVA0 specimen (40.20 MPa), respectively. After 200 freeze-thaw cycles, the strength of the specimen with 2.0% fiber content was 17.00% higher than that of the specimen with 1.0% fiber content. The strength loss rate increased with the increase in freeze-thaw cycles, and a higher fiber content resulted in a lower strength loss rate. After 50 freeze-thaw cycles, the strength loss rate of the specimen with 2.0% fiber content (9.43%) was 73.00% lower than that of the specimen with 0% fiber content (34.93%). After 200 freeze-thaw cycles, the strength loss rate of the specimen with 2.0% fiber content (30.26%) was 14.88% lower than that of the specimen with 1.0% fiber content (35.55%). The strength degradation rate of fiber-reinforced specimens accelerated in the later stage of freeze-thaw cycles (150–200 cycles). This is because the accumulation of freeze-thaw damage leads to the looseness of the internal structure, the decrease in bonding performance between fibers and the matrix, and the weakening of the bridging effect, which fails to effectively transfer stress, resulting in a rapid strength decline^[17].

The core mechanism of the cubic compressive strength degradation of PVA-ECC induced by freeze-thaw cycles is the accumulation of internal damage^[18]. During the freeze-thaw process, frost heave stress and osmotic pressure trigger the initiation and propagation of microcracks, destroying the integrity of the internal structure of the specimens, reducing the effective bearing area, and thus decreasing the compressive strength. Fiber-free specimens lack crack constraint, leading to rapid penetration of internal cracks and sharp strength degradation. PVA fibers restrict crack propagation through the bridging effect, disperse stress concentration, and enhance the integrity and ductility of the matrix, thereby reducing the impact of freeze-thaw damage on strength^[19]. In addition, the hydrophilicity of PVA fibers enables them to bond tightly with the matrix, fill some micro-pores, optimize the internal structure, and further improve the frost resistance and compressive performance of the material. A higher fiber content leads to more significant above-mentioned effects^[20].

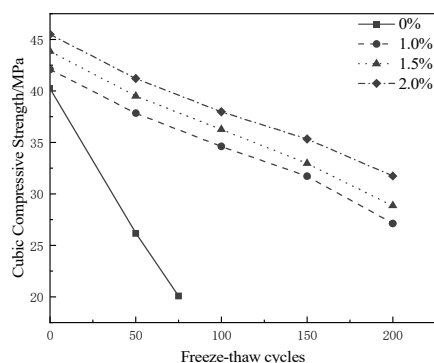


Figure 6. Variation of cubic compressive strength of PVA-ECC

4. Conclusion

(1) Freeze-thaw cycles aggravated the surface morphology damage of PVA-ECC, characterized by mortar spalling, fiber exposure, crack development, and corner damage. The fiber-free specimen fractured after 75 freeze-thaw cycles, while the fiber-reinforced specimens could withstand 200 freeze-thaw cycles and maintain overall integrity. PVA fibers restrict crack propagation via the bridging effect, significantly improving the frost-resistant appearance stability of the material.

(2) The mass loss rate of PVA-ECC increased with the increase in freeze-thaw cycles and decreased with the increase in fiber volume content. After 200 freeze-thaw cycles, the mass loss rate of the specimen with 2.0% fiber content was only 2.76%, which was 30.13% lower than that of the specimen with 1.0% fiber content. PVA fibers could effectively reduce mortar spalling and mass loss.

(3) The relative dynamic elastic modulus decreased with the increase in freeze-thaw cycles and increased with the increase in fiber volume content. After 200 freeze-thaw cycles, the relative dynamic elastic modulus of the specimen with 2.0% fiber content retained 73.19%, with a loss rate of only 26.81%. This indicates that a higher fiber content can inhibit the development of internal pores and cracks, maintaining the integrity of the material's internal structure.

(4) The cubic compressive strength degraded with the increase in freeze-thaw cycles and increased with the increase in fiber volume content. After 200 freeze-thaw cycles, the cubic compressive strength of the specimen with 2.0% fiber content was 31.73 MPa, with a strength loss rate of 30.26%. This was significantly lower than the strength loss rate (50.05%) of the fiber-free specimen after 75 freeze-thaw cycles. Through the bridging effect and structural optimization, PVA fibers effectively improved the compressive bearing capacity of the material after freeze-thaw cycles.

Acknowledgments

This is the place to fill in information about funds, sponsors, etc. that need to be thanked.

References

- [1] Li V C. On engineered cementitious composites (ECC) a review of the material and its applications[J]. *Journal of advanced concrete technology*, 2003, 1(3): 215-230.
- [2] Powers T C, Helmuth R A. Theory of volume changes in hardened portland-cement paste during freezing[C]//Highway research board proceedings. 1953, 32.
- [3] Zhang S, Zhao B. Research on the performance of concrete materials under the condition of freeze-thaw cycles[J]. *European journal of environmental and civil engineering*, 2013, 17(9): 860-871.
- [4] Tan Y, Xu Z, Liu Z, et al. Effect of silica fume and polyvinyl alcohol fiber on mechanical properties and frost resistance of concrete[J]. *Buildings*, 2022, 12(1): 47.
- [5] Li V C, Leung C K Y. Steady-state and multiple cracking of short random fiber composites[J]. *Journal of engineering mechanics*, 1992, 118(11): 2246-2264.
- [6] Shiping Y, Linli F, Shilang X, et al. Study on the bonding properties of the interface between ECC and thermal insulation materials under freeze-thaw environment[J]. *Construction and Building Materials*, 2022, 333: 127399.
- [7] Tosun Felekoğlu K, Gödek E. Role of matrix structure and flaw size distribution modification on deflection hardening behavior of polyvinyl alcohol fiber reinforced engineered cementitious composites (PVA-ECC)[J]. *Journal of Central South University*, 2019, 26(12): 3279-3294.
- [8] Ramezani M, Ozbulut O E, Sherif M M. Mechanical characterization of high-strength and ultra-high-performance engineered cementitious composites reinforced with polyvinyl alcohol and

- polyethylene fibers subjected to monotonic and cyclic loading[J]. *Cement and Concrete Composites*, 2024, 148: 105472.
- [9] Malhotra V M, Zhang M H, Read P H, et al. Long-term mechanical properties and durability characteristics of high-strength/high-performance concrete incorporating supplementary cementing materials under outdoor exposure conditions[J]. *Materials Journal*, 2000, 97(5): 518-525.
- [10] Nam J, Kim G, Lee B, et al. Frost resistance of polyvinyl alcohol fiber and polypropylene fiber reinforced cementitious composites under freeze thaw cycling[J]. *Composites Part B: Engineering*, 2016, 90: 241-250.
- [11] Cui Z, Dai F, Liu Y, et al. Dynamic fracture properties and criterion of cyclic freeze-thaw treated granite subjected to mixed-mode loading[J]. *Journal of Rock Mechanics and Geotechnical Engineering*, 2024, 16(12): 4971-4989.
- [12] Wu Q Y, Ma Q Y. Frost resistance and damage model of BSFC under Freeze-Thaw Cycles[J]. *J. Building Mater*, 2021, 24(06): 1169-1178.
- [13] Zhang J, Shu Y, Zhang J. Experimental study on dynamic and static mechanical properties of polyvinyl alcohol fiber cement soil under salt freezing cycle[J]. *Cold Regions Science and Technology*, 2024, 224: 104224.
- [14] Huang X, Wang T, Pang J, et al. Experimental study on the effect of freeze-thaw cycles on the apparent and mechanical properties of rubber concrete under chloride environment[J]. *Arabian Journal for Science and Engineering*, 2022, 47(4): 4133-4153.
- [15] Zhao X, Zheng L, Liu J, et al. Effect of moisture content on mechanical behavior of ultra-high toughness cementitious composites[J]. *Journal of Building Engineering*, 2023, 76: 107099.
- [16] Li Z, Wang X, Yan W, et al. Physical and mechanical properties of gypsum-based composites reinforced with basalt, glass, and PVA fibers[J]. *Journal of Building Engineering*, 2023, 64: 105640.
- [17] Li Y, Zhai Y, Liang W, et al. Dynamic mechanical properties and visco-elastic damage constitutive model of freeze-thawed concrete[J]. *Materials*, 2020, 13(18): 4056.
- [18] Li Y, Guo H, Zhou H, et al. Damage characteristics and constitutive model of concrete under uniaxial compression after Freeze-Thaw damage[J]. *Construction and Building Materials*, 2022, 345: 128171.
- [19] Li Y, Zhang Q, Wang R, et al. Experimental investigation on the dynamic mechanical properties and microstructure deterioration of steel fiber reinforced concrete subjected to freeze-thaw cycles[J]. *Buildings*, 2022, 12(12): 2170.
- [20] Song S, Niu Y, Zhong X. Study on dynamic mechanical properties of carbon nanotubes reinforced concrete subjected to freeze-thaw cycles[J]. *Structural Concrete*, 2022, 23(5): 3221-3233.